

Handling Large Discrete Action Spaces via Dynamic Neighborhood Construction

Fabian Akkerman*

University of Twente
f.r.akkerman@utwente.nl

Julius Luy*

Technical University of Munich
julius.luy@tum.de

Wouter van Heeswijk

University of Twente
w.j.a.vanheeswijk@utwente.nl

Maximilian Schiffer

Technical University of Munich
schiffer@tum.de

Abstract

Large discrete action spaces remain a central challenge for reinforcement learning methods. Such spaces are encountered in many real-world applications, e.g., recommender systems, multi-step planning, and inventory replenishment. The mapping of continuous proxies to discrete actions is a promising paradigm for handling large discrete action spaces. Existing continuous-to-discrete mapping approaches involve searching for discrete neighboring actions in a static pre-defined neighborhood, which requires discrete neighbor lookups across the entire action space. Hence, scalability issues persist. To mitigate this drawback, we propose a novel Dynamic Neighborhood Construction (DNC) method, which dynamically constructs a discrete neighborhood to map the continuous proxy, thus efficiently exploiting the underlying action space. We demonstrate the robustness of our method by benchmarking it against three state-of-the-art approaches designed for large discrete action spaces across three different environments. Our results show that DNC matches or outperforms state-of-the-art approaches while being more computationally efficient. Furthermore, our method scales to action spaces that so far remained computationally intractable for existing methodologies.

1 Introduction

In deep reinforcement learning (DRL), ample methods exist to successfully handle large state spaces, but methods to handle large discrete action spaces (LDAS) remain scarce [Dulac-Arnold et al., 2021]. Still, LDAS often arise when applying DRL to real-world applications, e.g., for recommender systems [Afsar et al., 2022], portfolio optimization [Pigorsch and Schäfer, 2021], or inventory replenishment problems [Boute et al., 2022]. The decision space for such problems is often discrete and suffers from a curse of dimensionality, e.g., managing the inventory replenishment for a group of N products with each having G different order levels yields an action space of size G^N . Off-the-shelf DRL algorithms – e.g., Deep Q-Networks (DQN) [Mnih et al., 2013], Deep Policy Gradients (DPG) [Silver et al., 2014], or Proximal Policy Optimization (PPO) [Schulman et al., 2017] – fail to handle such LDAS, as they require in- or output nodes for each discrete action, which renders learning accurate Q -values (in DQN) or action probabilities (in DPG or PPO) computationally intractable. To overcome this challenge, recent research suggests handling DRL problems with LDAS by learning a continuous policy and mapping its outputs to discrete actions [Dulac-Arnold et al., 2015, Chandak et al., 2019]. Although handling fairly large action spaces, these techniques rely on static, a priori

*Equal contribution.

specified neighborhoods to map actions, such that their scalability to very large LDAS remains limited.

Against this background, we propose a novel algorithmic pipeline that embeds continuous-to-discrete action mappings via dynamic neighborhood construction into an actor-critic algorithm. This pipeline overcomes the scalability issues of previous approaches, scaling up to action spaces of size 10^{73} , while showing comparable or even improved algorithmic performance.

Related Literature Factorization methods reduce the action space’s size by grouping actions and finding action representations for each grouping that are easier to learn. Sallans and Hinton [2004] and Pazis and Parr [2011] factorize the action space into binary subsets, evaluating binary actions for each subset to yield $\log(\mathcal{A})$ operations. Dulac-Arnold et al. [2012] combine action binarization with rollout classification policy iteration [Lagoudakis and Parr, 2003] to accelerate learning. More recently, papers enrich similarity groupings via expert demonstrations [Tennenholtz and Mannor, 2019], factor action spaces into tensors [Mahajan et al., 2021], or define symbolic representations of state-action values, using gradient-based search to derive actions [Cui and Khardon, 2016, 2018]. Tavakoli et al. [2018] consider value-based DRL for LDAS, incorporating the action space structure into the Q -network architecture to obtain an output layer that scales linearly with the action dimensionality. Similar works empirically test value function decomposition [Sharma et al., 2017], prove unbiasedness of Q -values when factorizing [Tang et al., 2022], and employ decomposition via action branching [Wei et al., 2020]. Although some of these works cover extremely large action spaces with as many as 2^{40} actions, the proposed approaches require an a priori encoding definition for each discrete action, confining these methods to enumerable action spaces.

Methods such as hierarchical reinforcement learning (HRL) and multi-agent reinforcement learning (MARL) effectively employ factorization as well. Kim et al. [2021b] apply HRL to NP-hard vehicle routing problems by generating candidate routes, which are subsequently decomposed into route-segments and solved to optimality. Zhang et al. [2020] reduce the evaluated action to a k -step adjacency action space based on the current state. Similarly, Kim et al. [2021a] only consider actions for promising *landmark* states, thereby reducing the number of decisions that need to be learned. Peng et al. [2021] use MARL to factorize centralized agents by dividing the joint action-value function into per-agent utilities and subsequently combine these in a central Q -learning update. Enders et al. [2022] consider large-scale autonomous vehicle dispatching and propose a decomposition, for which they generate each action space element independently and subsequently find a feasible global solution via bipartite matching. These methods prove to be effective on specific problem classes. However, they do not leverage the action space’s underlying continuous structure. Additionally, they frequently require substantial design- and parameter tuning effort, particularly in the case of MARL.

While factorization methods reduce the number of considered actions, continuous-to-discrete mappings consider the continuum between discrete actions in a first step, converting continuous actions to discrete ones in a second step. The work of Van Hasselt and Wiering [2007] uses an actor-critic algorithm, rounding the actor’s continuous output to the closest integer to obtain a discrete counterpart. Vanvuchelen et al. [2022] extend this concept to multi-dimensional action vectors, normalizing the actor’s output, and rounding it to the next discrete value. Such rounding techniques are straightforward and computationally efficient, but may yield unstable performance if their mapping is too coarse. Different continuous outputs might be mapped to the same discrete action, while ignoring potentially better neighbors. To mitigate this issue, Dulac-Arnold et al. [2015] replace the rounding step through a k -nearest neighbor search across \mathcal{A} , generating the entire action space \mathcal{A} a priori to preserve efficiency, and selecting the neighbor with the highest Q -value to obtain a discrete action. Wang et al. [2021] achieve faster learning by leveraging k -dimensional trees instead of a k -nearest neighbor search. The major drawback of these approaches is its limited scalability as they necessitate to define—and store—the complete discrete action space a priori, e.g., in the form of a matrix.

Another research stream aims at learning action representations. Thomas and Barto [2012] use a goal-conditioned policy to learn motor primitives, i.e., aggregated abstractions of lower level actions. Chandak et al. [2019] consider a policy gradient method, wherein the policy returns continuous actions in an embedding space and employ supervised learning to identify a unique embedding for each discrete action. Follow up works consider combined state-action embeddings [Whitney et al., 2020, Pritz et al., 2021], or reduce the impact of out-of-distribution actions in offline DRL by measuring behavioral and data-distributional relations between discrete actions [Gu et al., 2022]. Other works propose to learn an embedding for all feasible actions by means of a value-based

approach [He et al., 2016], or learn which actions to avoid by predicting suboptimal actions [Zahavy et al., 2018]. In general, learning action representations avoids an a priori definition of \mathcal{A} , but requires a vast amount of data to learn the respective representation, often hampering algorithmic performance. Moreover, scalability issues remain due to learning dedicated representations for each action.

As can be seen, existing methods to handle LDAS are limited in their general applicability due to one of the following obstacles: (i) straightforward factorization approaches require defining handcrafted encodings a priori and are consequently confined to enumerable action spaces, (ii) approaches that base on HRL or MARL overcome this obstacle but are highly problem-specific and lack generalizability, (iii) static continuous-to-discrete mappings lack scalability as they require to define—and store—the complete discrete action space a priori, triggering memory limitations for very large spaces, (iv) learning action representations overcomes this drawback but shows unstable performance across applications and suffers with respect to scalability due to learning dedicated representations for each action. Concluding, none of the approaches proposed to handle LDAS so far can be generically applied to a multitude of applications with (very) LDAS while providing state-of-the-art algorithmic performance.

Contribution To close the research gap outlined above, we propose a novel algorithmic pipeline that ensures generalized applicability to LDAS while maintaining or improving the state-of-the-art in solution quality and overcoming scalability issues of existing approaches. This pipeline embeds continuous-to-discrete action mappings via dynamic neighborhood construction (DNC) into an actor-critic algorithm. Specifically, we leverage DNC to convert the actor’s continuous output into a discrete action via a simulated annealing (SA) based search. To this end, we use discrete actions’ Q-values derived from the critic to guide the search. Although our approach classifies as a continuous-to-discrete action mapping, it does not require an a priori definition of the action space. Moreover, it is not problem-specific, and can generally be applied to problem settings solved with actor-critic algorithms. We benchmark our pipeline against various state-of-the-art approaches [Dulac-Arnold et al., 2015, Chandak et al., 2019, Vanvuchelen et al., 2022] and a vanilla actor critic (VAC) baseline across three environments depicting different application domains: an artificial maze environment and two real-world inspired environments by means of a recommender system and a joint inventory replenishment problem. Our results verify the superior performance of our pipeline: it scales up to discrete action spaces of size 10^{73} , vastly surpassing the action space size solved by existing approaches. Moreover, it shows comparable or improving solution quality across all investigated environments. Our code can be found at: <https://github.com/tumBAIS/dynamicNeighborhoodConstruction>

The paper’s remainder is as follows: Section 2 introduces our problem setting, while Section 3 details our methodology. We elaborate on our experimental design in Section 4 and discuss numerical results in Section 5. Section 6 concludes this paper with a short discussion and pointers to future work.

2 Problem Description

We study discrete, sequential decision-making problems formalized as Markov decision processes (MDPs), described by a state space \mathcal{S} , a discrete action space \mathcal{A} , a reward function $r: \mathcal{S} \times \mathcal{A} \rightarrow \mathbb{R}$, and transition dynamics $\mathbb{P}: \mathcal{S} \times \mathcal{A} \times \mathcal{S} \rightarrow [0, 1]$. We represent states $\mathbf{s} \in \mathcal{S}$ and actions $\mathbf{a} \in \mathcal{A}$ by N - and M -dimensional vectors, such that $\mathbf{a} \in \mathbb{N}^N$ and $\mathbf{s} \in \mathbb{R}^M$. Note that we consider multi-dimensional actions, represented as a vector, to emphasize general applicability. Still, we refer to this action vector as an action in the remainder of this paper for the sake of conciseness. Let us denote a policy by $\pi: \mathcal{S} \rightarrow \mathcal{A}$ and the state-action value function by $Q^\pi(\mathbf{s}, \mathbf{a}) = \mathbb{E}_\pi [\sum_{t=0}^{\infty} \gamma^t r_t | \mathbf{s}, \mathbf{a}]$, where $\gamma \in [0, 1)$ denotes the discount factor. We aim to find a policy that maximizes the objective function $J = \mathbb{E}_{\mathbf{a} \sim \pi} [Q^\pi(\mathbf{s}, \mathbf{a})]$.

To introduce our method, first consider an actor-critic framework, in which an actor determines action $\mathbf{a} \in \mathcal{A}$ based on a policy (actor network) π_θ parameterized by weight vector θ , and a critic parameterized by \mathbf{w} estimates the value of this action, i.e., returns $Q_w(\mathbf{s}, \mathbf{a})$. The actor is updated in the direction suggested by the critic by maximizing the objective function $J(\theta)$. The actor network’s output layer contains $|\mathcal{A}|$ nodes, each reflecting the probability of an action $\mathbf{a} \in \mathcal{A}$, i.e., the network $\pi_\theta(\mathbf{s})$ encodes the policy. In many real-world problems, $|\mathcal{A}|$ grows exponentially with the state dimension. In these cases, obtaining an accurate policy requires vast amounts of training data and exploration to ensure generalization over \mathcal{A} , making training of π_θ intractable.

To mitigate this drawback, we will solve the following surrogate problem in the remainder of this paper. Instead of finding a discrete policy returning action probabilities for each $\mathbf{a} \in \mathcal{A}$, we aim at finding a policy that returns continuous actions $\hat{\mathbf{a}} \in \mathbb{R}^N$ and a function $f(\hat{\mathbf{a}}) = \mathbf{a}$ that maps continuous actions to discrete ones. This approach yields several advantages. First, we can use off-the-shelf policy gradient algorithms to learn $\pi_\theta(\mathbf{s})$, as they perform well in continuous action spaces. Moreover, π_θ 's output layer now grows linearly with the number of entries in $\hat{\mathbf{a}}$.

3 Methodology

Figure 1 shows the rationale of our algorithm's pipeline, which builds upon an actor-critic framework, leveraging DNC to transform the actor's continuous output into a discrete action. Specifically, our pipeline comprises three steps. First, we use the actor's output $\hat{\mathbf{a}}$ to generate a discrete base action $\bar{\mathbf{a}} \in \mathcal{A}$. We then iterate between generating promising sets of discrete neighbors \mathcal{A}' , and evaluating those based on the respective Q -values taken from the critic. Here, we exploit the concept of SA [cf. Kochenderfer and Wheeler, 2019] to guide our search and ensure sufficient exploration of potential neighborhoods. The remainder of this section details each step of our DNC procedure and discusses our algorithmic design decisions.

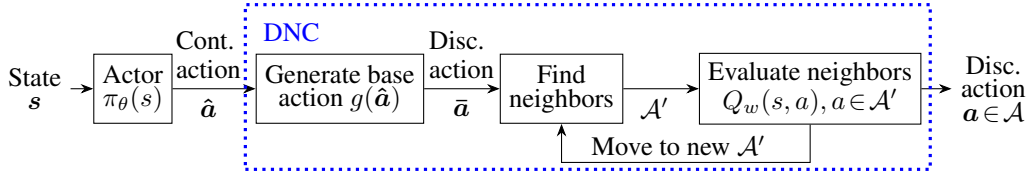


Figure 1: Pipeline for finding discrete actions in LDAS

Generating Discrete Base Actions We consider an actor network whose output corresponds to the first $\mu_\theta(\mathbf{s})_n \in \mathbb{R}$ and second $\sigma_\theta(\mathbf{s})_n \in \mathbb{R}$ order moments of pre-specified distributions for each element $n \in \{1, \dots, N\}$ of the action vector to parameterize a stochastic policy $\pi_\theta(\mathbf{s})$ with continuous actions $\hat{\mathbf{a}}$. After obtaining a continuous action $\hat{\mathbf{a}}$, we obtain a corresponding discrete base action $\bar{\mathbf{a}}$ by means of a function $g: \mathbb{R}^N \rightarrow \mathcal{A}$ that maps $\hat{\mathbf{a}}$ to the next feasible discrete action in \mathcal{A} as

$$g(\hat{a}_n) = \left\lfloor \frac{\text{clip}(\hat{a}_n) - c_{\min}}{c_{\max} - c_{\min}} \cdot (a_{\max} - a_{\min}) + a_{\min} \right\rfloor$$

with

$$\text{clip}(\hat{a}_n) = \begin{cases} c_{\min}, & \text{if } \hat{a}_n < c_{\min}, \\ c_{\max}, & \text{if } \hat{a}_n > c_{\max}, \\ \hat{a}_n, & \text{otherwise,} \end{cases}$$

denoting a clipping function. Similar to Vanvuchelen et al. [2022], we normalize the clipped action vector's entries \hat{a}_n to intervals with endpoints $c_{\min} \in \mathbb{R}$ and $c_{\max} \in \mathbb{R}$ respectively; linearly scale them to the range $[a_{\min}, a_{\max}]$, where a_{\min} and a_{\max} represent minimum and maximum values of \mathbf{a} 's individual entries; and finally round each entry to the nearest discrete counterpart. To this end, we note that $c_{\min} \in \mathbb{R}$ and $c_{\max} \in \mathbb{R}$ remain hyperparameters whose choice depends on the actor network's output layer. We refer to the supplementary material for a discussion on the impact and parameterization of c_{\min} and c_{\max} .

Generating Sets of Discrete Neighbors Within DNC, we aim to leverage neighbors of discrete base actions, motivated by the rationale that neighborhoods of actions exhibit a certain degree of cohesion. Specifically, when generating action neighborhoods \mathcal{A}' , we premise that (i) action pairs with small vector distances generate similar Q -values, and (ii) the action space is (locally) structured.

Definition 1 We measure action similarity within \mathcal{A}' via a Lipschitz constant L satisfying $|Q^\pi(\mathbf{s}, \mathbf{a}) - Q^\pi(\mathbf{s}, \mathbf{a}')| \leq L \|\mathbf{a} - \mathbf{a}'\|_2$ for all $\mathbf{a}, \mathbf{a}' \in \mathcal{A}'$.

Lemma 1 Action similarity L is given by $\sup_{\mathbf{a}, \mathbf{a}' \in \mathcal{A}', \mathbf{a} \neq \mathbf{a}'} \frac{|Q^\pi(\mathbf{s}, \mathbf{a}) - Q^\pi(\mathbf{s}, \mathbf{a}')|}{\|\mathbf{a} - \mathbf{a}'\|_2}$, ensuring that $|Q^\pi(\mathbf{s}, \mathbf{a}) - Q^\pi(\mathbf{s}, \mathbf{a}')| \leq L \|\mathbf{a} - \mathbf{a}'\|_2$ for all $\mathbf{a}, \mathbf{a}' \in \mathcal{A}'$.

To prove Lemma 1, we use that \mathcal{A}' is discrete and finite and maps onto the real domain, $J(\theta)$ is Lipschitz continuous, and thus a finite L exists. We refer to the supplementary material for the proof.

To generate discrete neighbors of \bar{a} , we perturb each action vector entry \bar{a}_n , $n \in \{1, \dots, N\}$. To do so, we define a perturbation matrix $\mathbf{P} = (P_{ij})_{i=1, \dots, N; j=1, \dots, 2dN}$, with d being the neighborhood depth. Moreover, let ϵ denote a scaling constant, that allows us to look at more distant (higher ϵ) or closer (smaller ϵ) neighbors. With this notation, the perturbation matrix \mathbf{P} reads as follows

$$P_{ij} = \begin{cases} \epsilon (\lfloor (j-1)/N \rfloor + 1), & \text{if, } j \in \{i, i+N, i+2N, \dots, i+(d-1)N\}, \\ -\epsilon (\lfloor (j-1)/N \rfloor + 1 - d), & \text{if, } j \in \{i+dN, i+(d+1)N, \dots, i+(2d-1)N\}, \\ 0, & \text{otherwise.} \end{cases}$$

The first $d \cdot N$ columns of \mathbf{P} are vectors with one non-zero entry describing a positive perturbation of each entry in \bar{a} , the last $d \cdot N$ columns describe negative perturbations. Let $\bar{\mathbf{A}} = (\bar{A}_{ij})_{i=1, \dots, N; j=1, \dots, 2dN}$ denote a matrix that stores \bar{a} in each of its columns. We then obtain the perturbed matrix $\mathbf{A} = (A_{ij})_{i=1, \dots, N; j=1, \dots, 2dN}$ as

$$\mathbf{A} = \bar{\mathbf{A}} + \mathbf{P},$$

such that \mathbf{A} 's columns form the set \mathcal{A}' , yielding $2 \cdot N \cdot d$ neighbors with maximum L_2 distance $(d\epsilon)$.

Note that this perturbation approach allows for efficient implementation and scales to very large action spaces by design as it limits the exploration of the neighborhood of \bar{a} , which in a general case would still increase exponentially with respect to maximum L_2 -distance of $\leq (d\epsilon)$. Clearly, limiting the neighborhood evaluation may incur a performance loss, but we argue that this loss is limited, as our search process described in the next section is able to recover initially ignored neighbors.

Assuming that an action's structured neighborhood relates to a locally convex $J(\theta)$, we can show that the worst-case performance relative to base action \bar{a} is bound within a radius corresponding to the maximum perturbation distance, i.e., $(d\epsilon)$. To formalize this, let $\mathcal{A}'' = \{\mathbf{a} \in \mathcal{A}' : \|\mathbf{a} - \bar{a}\|_2 = (d\epsilon)\}$ denote the set of maximally perturbed actions with respect to \bar{a} .

Lemma 2 *If $J(\theta)$ is locally upward convex for neighborhood \mathcal{A}' with maximum perturbation $(d\epsilon)$ around base action \bar{a} , then worst-case performance with respect to \bar{a} is bound by the maximally perturbed actions $\mathbf{a}'' \in \mathcal{A}''$ via $Q^\pi(\mathbf{s}, \mathbf{a}') \geq \min_{\mathbf{a}'' \in \mathcal{A}''} Q^\pi(\mathbf{s}, \mathbf{a}'')$, $\forall \mathbf{a}' \in \mathcal{A}'$.*

To prove Lemma 2 we leverage that inequality $\min_{\mathbf{a}'' \in \mathcal{A}''} Q^\pi(\mathbf{s}, \mathbf{a}'') \leq Q^\pi(\mathbf{s}, \lambda(\mathbf{a}) + (1-\lambda)(\mathbf{a}'))$, with $\mathbf{a}, \mathbf{a}' \in \mathcal{A}''$ and $\lambda \in [0, 1]$, holds by definition of upward convexity and refer to the supplementary material for a complete proof.

Evaluating Discrete Action Neighborhoods Algorithm 1 details the evaluation of a base action's neighborhood and our final selection of the discrete action \mathbf{a} that we map to $\hat{\mathbf{a}}$. We initially select the discrete action within a neighborhood that yields the highest Q -value. However, our selection does not base on a single neighborhood evaluation, but employs an iterative SA-based search scheme to efficiently explore various neighborhoods. SA is an efficient probabilistic search technique that facilitates to escape local optima during a search by occasionally accepting worse actions than the best one found [cf. Kochenderfer and Wheeler, 2019].

Specifically, Algorithm 1 works as follows. After generating a set of neighbors \mathcal{A}' (1.3), we utilize the critic to obtain Q -values for $\mathbf{a}' \in \mathcal{A}'$, which includes the current base action \bar{a} and each neighbor (1.4). Subsequently, we store the k -best neighbors in an ordered set $\mathcal{K}' \subseteq \mathcal{A}'$ and store \mathcal{K}' in \mathcal{K} , the latter set memorizing all evaluated actions thus far (1.5). From \mathcal{K}' , we select action \mathbf{k}_1 , which by definition of \mathcal{K}' has the highest associated Q -value, for evaluation (1.6). If the Q -value of $\mathbf{k}_1 \in \mathcal{K}'$ exceeds the Q -value of the base action \bar{a} , we accept \mathbf{k}_1 as new base action \bar{a} (1.8). If it also exceeds the current best candidate action, \bar{a}^* (1.10), we accept it as the new best candidate action. If the action \mathbf{k}_1 does not exhibit a higher Q -value than \bar{a} , we accept it with probability $1 - \exp[-(Q_w(\bar{a}) - Q_w(\mathbf{k}_1))/\beta]$ and reduce β by cooling parameter c_β (1.12), or reject it and move to a new base action, sampled from \mathcal{K} (1.14). Finally, the parameter k is reduced by cooling parameter c_k . Steps (1.3) to (1.15) are repeated until the stopping criterion (1.2) has been met. We then set $\mathbf{a} = \bar{a}^*$, i.e., we use the action with the highest Q -value found as our final discrete action. For a more detailed description of the search process and its hyperparameter tuning, we refer to the supplementary material.

Algorithm 1 Dynamic Neighborhood Construction

```
1: Initialize  $k, \beta, c_\beta$ , and  $c_k$ ,  $\bar{a} \leftarrow g(\hat{a})$ ,  $\bar{a}^* \leftarrow \bar{a}$ ,  $\mathcal{K} = \emptyset$ 
2: while  $k > 0$ , or  $\beta > 0$  do
3:   Find neighbors  $\mathcal{A}'$  to  $\bar{a}$  with  $P_{ij}$ 
4:   Get  $Q$ -values for all neighbors in  $\mathcal{A}'$ 
5:   Obtain set  $\mathcal{K}'$  with  $k$ -best neighbors,  $\mathcal{K} \leftarrow \mathcal{K} \cup \mathcal{K}'$ 
6:    $\mathbf{k}_1 \leftarrow \mathcal{K}'$ , with  $\mathbf{k}_1 = \arg \max_{\mathbf{k} \in \mathcal{K}'} Q_w(s, \mathbf{k})$ 
7:   if  $Q_w(s, \mathbf{k}_1) > Q_w(s, \bar{a})$  then
8:     Accept  $\mathbf{k}_1 \in \mathcal{K}'$ ,  $\bar{a} \leftarrow \mathbf{k}_1$ 
9:     if  $Q_w(s, \mathbf{k}_1) > Q_w(s, \bar{a}^*)$  then
10:        $\bar{a}^* \leftarrow \mathbf{k}_1$ 
11:   else if  $\text{rand}() < \exp[-(Q_w(\bar{a}) - Q_w(\mathbf{k}_1)) / \beta]$  then
12:     Accept  $\mathbf{k}_1 \in \mathcal{K}'$ ,  $\bar{a} \leftarrow \mathbf{k}_1$ ,  $\beta \leftarrow \beta - c_\beta$ 
13:   else
14:     Reject  $\mathbf{k}_1 \in \mathcal{K}'$ ,  $\bar{a} \leftarrow \mathbf{k}_{\text{rand}} \in \mathcal{K}$ 
15:      $k \leftarrow \lceil k - c_k \rceil$ 
16: Return  $\bar{a}^*$ 
```

Discussion A few technical comments on the design of our algorithmic pipeline are in order.

First, a composed policy of the form $\mathbf{a} = \pi'_\theta(s) = \text{DNC}(\pi_\theta(s))$ is not fully differentiable. However, we argue that DNC’s impact can be interpreted as a non-deterministic aspect of the environment. To ensure that our overall policy’s backpropagation works approximately, we follow two steps, similar to Dulac-Arnold et al. [2015]. Step 1 bases the actor’s loss function on the continuous action \hat{a} . This has the advantage of exploiting information from the continuous action space, that would have been lost if we had trained the actor on the discrete action \hat{a} . Step 2 trains the critic using the discrete action \mathbf{a} , i.e., the actions that were applied to the environment and upon which rewards were observed. We detail the integration of DNC into an actor-critic algorithm in the supplementary material.

Second, mapping a continuous action to the most suitable discrete neighbor can be challenging, especially when considering reward variance. We hypothesize that the critic smooths out noise through its Q -values, allowing to differentiate neighboring actions better than the actor could via exploration. Hence, we presume that DNC works best for problems that exhibit (i) a certain degree of reward variance, (ii) a structured action space, and (iii) a certain degree of similarity among neighbors.

Third, one may argue that using an iterative SA-based algorithm is superfluous as our overall algorithmic pipeline already utilizes a stochastic policy π_θ , which ensures exploration. Here, we note that utilizing π_θ only ensures exploration in the continuous action space. To ensure that subsequent deterministic steps in \mathcal{A} , i.e., base action generation and neighborhood selection, do not lead to local optima, we use SA to efficiently search across different and potentially better neighborhoods. In fact, we can show that with the chosen algorithmic design, DNC leads to improving actions in finite time.

Lemma 3 *Consider a neighborhood \mathcal{A}' and improving actions satisfying $Q^\pi(s, \mathbf{a}) > \max_{\mathbf{a}' \in \mathcal{A}'} Q^\pi(s, \mathbf{a}')$, $\mathbf{a} \in \mathcal{A} \setminus \mathcal{A}'$. In finite time, DNC will accept improving actions, provided that (i) β and k cool sufficiently slowly and (ii) a maximum perturbation distance ($d\epsilon$) is set such that all action pairs can communicate.*

To prove Lemma 3, we utilize that under conditions (i) and (ii), our SA-based search can be formalized as an irreducible and aperiodic Markov chain over \mathcal{A} . A positive transition probability then applies to each action pair. For a complete proof, we refer to the supplementary material.

4 Experimental Design

We compare the performance of our algorithmic pipeline (DNC) against four benchmarks: a vanilla actor-critic algorithm (VAC), the static MinMax mapping proposed in Vanvuchelen et al. [2022], the k -nearest neighbors (k nn) mapping proposed in Dulac-Arnold et al. [2015], and the learned action representation (LAR) approach proposed in Chandak et al. [2019]. To this end, VAC can be seen as a

baseline, while MinMax, knn, and LAR denote state-of-the-art benchmarks. We detail all of these benchmarks and respective hyperparameter tuning in the supplementary material.

We consider three different environments to rigorously analyze algorithmic performance, which we summarize in the following. For details on their implementation as well as the databases used, we refer to the supplementary material.

First, we consider a maze environment [cf. Chandak et al., 2019], in which an agent needs to navigate through a maze, avoiding obstructions and finding a goal position. The agent receives continuous coordinates on its location as input and decides on the activation of N actuators, equally spaced around the agent. The actuators move the agent in the direction they are pointing at. The resulting action space is exponential in the number of actuators, i.e., $|\mathcal{A}| = 2^N$. The agent incurs a small negative reward for each step and a reward of 100 when the goal is reached. Random noise of 10% is added to every action.

Second, we study a recommender system [cf. Dulac-Arnold et al., 2015], which suggests d items, each with a unique reward, out of a large pool of B items to a customer. Here, the action space size is $|\mathcal{A}| = \binom{B}{d}$. The customer selects either one of the suggested or a random item. The episode ends with probability 0.1 if the user picks the recommended item or with a probability of 0.2 otherwise. We construct the environment using data from the MovieLens 25M Dataset [Grouplens, 2023], considering 1639 movies, and attribute a feature vector of size $N = 23$ to each movie. Hence, action vectors have the size $N = 23$, when recommending one and $N = 46$ when recommending two items. We simulate probabilities of picking certain recommended items based on the similarity between the last item the customer picked and the recommended one. We detail the design of the similarity measure in the supplementary material.

Third, we consider a joint inventory replenishment problem [cf. Vanvuchelen et al., 2022]. Consider a retailers' warehouse that stocks N items $i \in \mathcal{I}$. Each timestep, customer demand is served from the warehouse stock and the retailer needs to decide on the ordering quantity, aiming to minimize total costs that comprise per-item ordering costs o_i , holding costs h_i , and backorder costs b_i . The latter constitute a penalty for not being able to directly serve demand from stock in a time step. All individual items i are linked together through a common order costs O . This fixed cost term is incurred whenever at least one item is ordered, i.e., this term ensures that all items need to be considered simultaneously, since batch-reordering of multiple items is less costly. To ensure the decision space is finite, we let the agent decide on *order-up-to levels*, which are bound by S_{\max} , i.e., S_{\max} represents the maximum of items the retailer can stock. Hence, $|\mathcal{A}| = (S_{\max} + 1)^N$, which includes ordering 0 items. For all our experiments we set S_{\max} to 66, i.e., $|\mathcal{A}| = 67^N$.

5 Numerical Results

The following synthesizes the findings of our numerical studies, focusing on the scalability and algorithmic performance of each method. All results reported correspond to runs with the best hyperparameters found for each method, executed over 10 seeds. We refer to the supplementary material for detailed results as well as for profound information on the hyperparameter tuning.

Table 1 summarizes the learning performance of all algorithms across all three environments for varying action space sizes. To this end, a checkmark indicates that an algorithm was capable of robustly learning a performant policy for every instance within the respective action space size, a circle indicates that an algorithm could learn a (less) performant policy for some instances within the respective action space size, and a minus indicates that an algorithm failed to learn a performant policy on any instance of the respective action space size. Unsurprisingly, VAC already struggles

Table 1: Learning performance across all environments for different action space sizes $|\mathcal{A}|$.

	VAC	LAR	knn	MinMax	DNC
$10^3 < \mathcal{A} \leq 10^6$	○	✓	✓	✓	✓
$10^6 < \mathcal{A} \leq 10^9$	-	-	○	○	✓
$ \mathcal{A} \gg 10^9$	-	-	-	○	✓

to learn a performant policy for action spaces with a few thousand actions across the studied environments. While this observation generally supports the need for advanced methodologies to handle LDAS, it also verifies that the chosen environments and their resulting action spaces constitute sufficiently challenging benchmarks. Both the LAR and knn approach allow to learn policies for action spaces with a few thousand actions but fail on learning action spaces with $10^9 > |\mathcal{A}|$ as both require enumerable action spaces. For $10^6 < |\mathcal{A}| \leq 10^9$, knn learns performant policies in some environments, while LAR already fails to learn performant policies, caused by two combined factors. First, LAR needs to learn an embedding for each action from scratch. Second, often also the size of the action vector increases such that LAR does not only need to learn an increasing number of embeddings, but also a more complex target action vector representation. Only our DNC-based algorithm succeeds in robustly learning performant policies for all analyzed action space sizes, which highlights its superior scalability. The MinMax approach struggles to learn performant policies for instances with $|\mathcal{A}| > 10^9$, because it is susceptible to get stuck in local optima as the action space grows.

The remainder of this section focuses on algorithmic performance, i.e., the average performance during testing. Here, we omit the analyses of algorithms that are not capable of learning performant policies at all for the respective environments. To this end, Figure 2 shows the expected test return evaluated after a different number of training iterations and averaged over 10 random seeds. We log the policy 1000 times during training to perform test evaluations.

The left column depicts the results for the Maze environment. We observe that VAC is unable to find a good policy already for a “smaller” action spaces of size 2^{12} ($> 4k$ actions) actions. The other algorithms do not differ significantly in their performance. We note however that DNC requires more iterations to learn than knn and LAR and by design exhibits higher variance. DNC performs a search process that includes random search steps, and is hence prone to higher variance. When considering 2^{28} actions, we observe that only DNC and MinMax are able to learn a performant policy that is close to the goal of 100. All other algorithms run out of memory before starting the training process, as they require to either define the action space a priori (knn , VAC) or learn an embedding for every

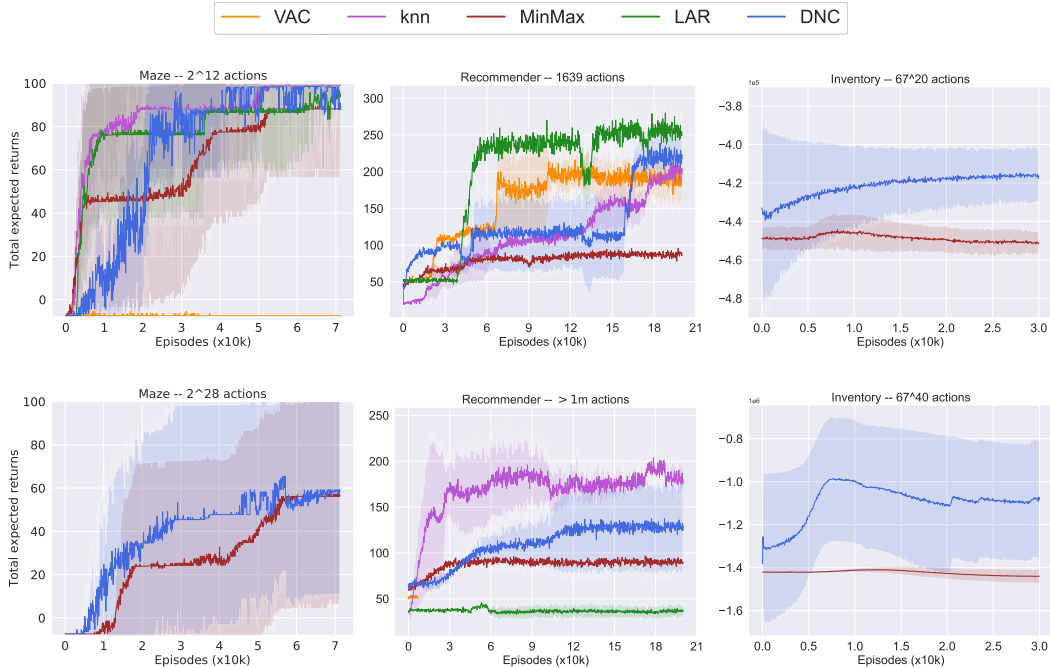


Figure 2: Average total expected returns during testing over 10 random seeds depending on the number of training iterations. The shaded area corresponds to the training seed variance corridor of 2 standard deviations. (Top) smaller action space variants of the three studied environments. (Bottom) larger action space variants for the three studied environments.

single action (LAR). We note that for this relatively simple environment with low reward variance, the benefit of considering neighbors to \hat{a} is limited, such that DNC does not outperform MinMax but obtains a similar performance. Hence, if continuous actions can already be accurately mapped to discrete ones, evaluating neighbors has limited added value.

The middle column of Figure 2 summarizes the results for the Recommender environment. When considering one recommended item (i.e., 1639 actions) VAC, k nn, LAR, and DNC show comparable performance after 200k training episodes, whereas MinMax fails to learn a performant policy. We observe that k nn and DNC are able to maintain performance as the action space increases beyond one million actions when considering two recommended items. In this setting, VAC fails since it only completes 5k training iterations before reaching the time limit, whereas LAR fails to learn a policy within 200k episodes. The sudden decrease in performance of LAR is caused by the increase in action space and action vector dimensions, requiring to learn a much larger number of embeddings in a more complex action space. Moreover, we clearly observe the advantages of using DNC compared to MinMax. As the recommender environment presents more inherent variance and non-linear behavior, it is beneficial to consider neighboring actions, i.e., recommended items. Thus, the neighborhood exploration as conducted by k nn and DNC is useful in this environment. We note that DNC’s variance across random seeds is comparatively high compared to k nn, owed to DNC’s inherent randomness.

The right column of Figure 2 reports results on the Inventory environment. As can be seen, only DNC is able to learn a performant policy for this environment. While k nn and LAR simply run out of memory, MinMax does not learn a performant policy. Similar to the recommender environment, the inventory environment exhibits non-linear behavior such as reward fluctuations due to joint order costs and demand uncertainty. Therefore, simple rounding and linear scaling to the next best discrete action as applied when using MinMax does not yield a converging learning behavior and consequently does not result in a performant policy.

To summarize the experimental findings, DNC is either competitive with or outperforms state-of-the-art benchmarks across all environments. It matches best performance for simple reward structures and offers competitive results when compared to k nn and LAR – which both employ powerful learning representations in their own right – on more complex structures and enumerable action spaces. The latter two methods, however, do not scale beyond enumeration. For very large action spaces DNC showcases unique performance, strongly outperforming its only viable benchmark MinMax in environments that exhibit a higher degree of reward variance.

6 Conclusion

In this paper, we present a novel algorithmic pipeline for deep reinforcement learning in environments with large discrete action spaces. Specifically, we propose a Dynamic Neighborhood Construction (DNC) that enables to integrate an effective continuous-to-discrete action mapping in an actor critic algorithm. Existing algorithms only perform well on medium to large action spaces, but cannot scale to non-enumerable action spaces as they either require a priori encodings of the action space, lack generalizability, or require to store the entire action space in-memory. In this context, our algorithmic pipeline shows two crucial advantages. First, it does not require enumerating the full action space, nor does it require storing the action space in-memory during the training process. Second, it only requires minimal problem-specific knowledge to generalize across problem classes. We compare our approach against various state-of-the-art benchmarks across three different environments: a maze environment, a recommender system environment, and an inventory replenishment environment. Our results verify the superior performance of our pipeline: it scales up to discrete action spaces of size 10^{73} , vastly surpassing the action space size solved by existing approaches. Moreover, it shows comparable or improving solution quality across all investigated environments.

Our algorithmic pipeline performs particularly well in cases where (i) the explored discrete action counterparts are not too far away from the respective continuous action to ensure performance bounds and justify differentiation; and (ii) a certain degree of action space structure and similarity between actions exists, which implies a spectrum of reward variance on which the added value of neighborhood search depends. While these characteristics constitute limitations of our work, they at the same time hold true for many online decision making environments in industry and practice. The promising results of DNC motivate future work to explore extending of our pipeline to alternative neighborhood

operators and selection criteria, deploying a PPO actor to enforce trusted action neighborhoods, or using graph neural networks to efficiently evaluate neighborhoods.

Acknowledgments and Disclosure of Funding

We would like to thank Yash Chandak for sharing his code and for answering our questions considering the learned action representation LAR method [Chandak et al., 2019]. Our code for the LAR benchmark meaningfully builds upon and extends his codebase.

Supplementary Material

A Proofs of Lemmata 1, 2, and 3

Lemma 1 Action similarity L is given by $\sup_{\mathbf{a}, \mathbf{a}' \in \mathcal{A}', \mathbf{a} \neq \mathbf{a}'} \frac{|Q^\pi(\mathbf{s}, \mathbf{a}) - Q^\pi(\mathbf{s}, \mathbf{a}')|}{\|\mathbf{a} - \mathbf{a}'\|_2}$, ensuring that $|Q^\pi(\mathbf{s}, \mathbf{a}) - Q^\pi(\mathbf{s}, \mathbf{a}')| \leq L \|\mathbf{a} - \mathbf{a}'\|_2$ for all $\mathbf{a}, \mathbf{a}' \in \mathcal{A}'$.

Proof Since the action neighborhood \mathcal{A}' is finite and discrete, there exists a minimum Euclidean distance $\delta > 0$ between any two distinct actions $\mathbf{a}, \mathbf{a}' \in \mathcal{A}'$, i.e., $\|\mathbf{a} - \mathbf{a}'\|_2 \geq \delta$ for $\mathbf{a} \neq \mathbf{a}'$.

Consider any two distinct actions $\mathbf{a}, \mathbf{a}' \in \mathcal{A}'$ and their corresponding Q -values $Q^\pi(\mathbf{s}, \mathbf{a}) \in \mathbb{R}$ and $Q^\pi(\mathbf{s}, \mathbf{a}') \in \mathbb{R}$, with state \mathbf{s} fixed. By the triangle inequality, we have:

$$\begin{aligned} 0 &\leq \\ |Q^\pi(\mathbf{s}, \mathbf{a}) - Q^\pi(\mathbf{s}, \mathbf{a}')| &= \\ |Q^\pi(\mathbf{s}, \mathbf{a}) + (-Q^\pi(\mathbf{s}, \mathbf{a}'))| &\leq \\ |Q^\pi(\mathbf{s}, \mathbf{a})| + |-Q^\pi(\mathbf{s}, \mathbf{a}')| &= \\ |Q^\pi(\mathbf{s}, \mathbf{a})| + |Q^\pi(\mathbf{s}, \mathbf{a}')| &. \end{aligned}$$

Let $Q^{\max} = \max_{\mathbf{a} \in \mathcal{A}'} Q^\pi(\mathbf{s}, \mathbf{a})$ be the maximum Q -value over all actions in \mathcal{A}' . From the triangle inequality, it follows that $|Q^\pi(\mathbf{s}, \mathbf{a}) - Q^\pi(\mathbf{s}, \mathbf{a}')| \leq 2Q^{\max}$ must hold.

Now, for any action pair $\mathbf{a} \neq \mathbf{a}'$, we have $\|\mathbf{a} - \mathbf{a}'\|_2 \geq \delta$ and $|Q^\pi(\mathbf{s}, \mathbf{a}) - Q^\pi(\mathbf{s}, \mathbf{a}')| \leq 2Q^{\max}$. Hence, the ratio $\frac{|Q^\pi(\mathbf{s}, \mathbf{a}) - Q^\pi(\mathbf{s}, \mathbf{a}')|}{\|\mathbf{a} - \mathbf{a}'\|_2}$ is a non-negative real number bounded by $\frac{2Q^{\max}}{\delta}$ for all $\mathbf{a}, \mathbf{a}' \in \mathcal{A}'$ satisfying $\mathbf{a} \neq \mathbf{a}'$. Since the action space is finite, the number of ratios is also finite, and we bound the Lipschitz constant:

$$L = \sup_{\mathbf{a}, \mathbf{a}' \in \mathcal{A}', \mathbf{a} \neq \mathbf{a}'} \frac{|Q^\pi(\mathbf{s}, \mathbf{a}) - Q^\pi(\mathbf{s}, \mathbf{a}')|}{\|\mathbf{a} - \mathbf{a}'\|_2} \leq \frac{2Q^{\max}}{\delta} .$$

Hence, L exists and is finite, providing a measure on action similarity. \square

Lemma 2 If $J(\theta)$ is locally upward convex for neighborhood \mathcal{A}' with maximum perturbation ($d \in$) around base action $\bar{\mathbf{a}}$, then worst-case performance with respect to $\bar{\mathbf{a}}$ is bound by the maximally perturbed actions $\mathbf{a}'' \in \mathcal{A}''$ via $Q^\pi(\mathbf{s}, \mathbf{a}') \geq \min_{\mathbf{a}'' \in \mathcal{A}''} Q^\pi(\mathbf{s}, \mathbf{a}'')$, $\forall \mathbf{a}' \in \mathcal{A}'$.

Proof Evaluating $\arg \max_{\mathbf{a} \in \mathcal{A}} Q_w(\mathbf{s}, \mathbf{a})$ may return any $\mathbf{a} \in \mathcal{A}'$, as Q_w might have arbitrary values.

Therefore, we must prove that the performance bound holds for all $\mathbf{a} \in \mathcal{A}'$. Via the local convexity of $J(\theta)$ around base action $\bar{\mathbf{a}}$, we prove that worst-case performance is bound by a maximally perturbed action in \mathcal{A}'' .

Let $\lambda \in [0, 1]$, $\mathbf{a}'', \mathbf{a}''', \mathbf{a}'''' \in \mathcal{A}''$ and $\mathbf{a}' \in \mathcal{A}'$. By definition of upward convexity, the following inequalities are satisfied.

$$\begin{aligned}
& \min_{\mathbf{a}'' \in \mathcal{A}''} Q^\pi(\mathbf{s}, \mathbf{a}'') = \\
& \lambda \min_{\mathbf{a}'' \in \mathcal{A}''} Q^\pi(\mathbf{s}, \mathbf{a}'') + (1-\lambda) \min_{\mathbf{a}''' \in \mathcal{A}'''} Q^\pi(\mathbf{s}, \mathbf{a}''') \leq \\
& \lambda Q^\pi(\mathbf{s}, \mathbf{a}''') + (1-\lambda) Q^\pi(\mathbf{s}, \mathbf{a}''''') \leq \\
& Q^\pi(\mathbf{s}, \lambda(\mathbf{a}''') + (1-\lambda)(\mathbf{a}''''')) .
\end{aligned}$$

This result holds $\forall \lambda \in [0, 1]$ and all maximally perturbed actions. Now, we only need to prove that $\forall \mathbf{a}' \in \mathcal{A}' \exists (\lambda, \mathbf{a}''', \mathbf{a}''''')$ such that $\mathbf{a}' = \lambda \mathbf{a}''' + (1-\lambda) \mathbf{a}'''''$, i.e., that linear combination of maximally perturbed actions can express all feasible actions $\mathbf{a}' \in \mathcal{A}'$.

Let us express neighbors via $\mathbf{a}' = \bar{\mathbf{a}} + \mathbf{P}_j$ for some $j \in \{1, \dots, 2Nd\}$. Moreover, let $j^+ \in \{Nd - (N-1), \dots, Nd\}$ be column indices corresponding to maximally positively perturbed actions and let $j^- \in \{2Nd - (N-1), \dots, 2Nd\}$ correspond to maximally negatively perturbed actions, and let l be the index of the non-zero entry of \mathbf{P}_j . Then, consider the maximally perturbed actions $\mathbf{A}_{j^+}^l, \mathbf{A}_{j^-}^l$, who only differ from $\bar{\mathbf{a}}$ on their l th element. We can now express \mathbf{a}' as

$$\mathbf{a}' = \lambda \mathbf{A}_{j^+}^l + (1-\lambda) \mathbf{A}_{j^-}^l. \quad (1)$$

Here, we obtain the required λ by solving Equation (1) for λ , for which we use the relevant perturbed entry P_{lj} . Solving the equation leads to $\lambda = \frac{P_{lj} + d\epsilon}{2d\epsilon}$, yielding a value between 0 and 1 as $-(d\epsilon) \leq P_{lj} \leq (d\epsilon)$. Therefore, we can express all neighbors $\mathbf{a}' \in \mathcal{A}'$ as linear combinations of maximally perturbed actions; hence, $\min_{\mathbf{a}'' \in \mathcal{A}''} Q^\pi(\mathbf{s}, \mathbf{a}'') \leq Q^\pi(\mathbf{s}, \mathbf{a}')$, $\forall \mathbf{a}' \in \mathcal{A}'$. \square

Lemma 3 Consider a neighborhood \mathcal{A}' and improving actions satisfying $Q^\pi(\mathbf{s}, \mathbf{a}) > \max_{\mathbf{a}' \in \mathcal{A}'} Q^\pi(\mathbf{s}, \mathbf{a}')$, $\mathbf{a} \in \mathcal{A} \setminus \mathcal{A}'$. In finite time, DNC will accept improving actions, provided that (i) β and k cool sufficiently slowly and (ii) a maximum perturbation distance ($d\epsilon$) is set such that all action pairs can communicate.

Proof The proof is structured into three steps: first, we show that DNC's simulated annealing procedure behaves as a non-homogeneous Markov chain that searches over the action space. We then show that this Markov chain is aperiodic and irreducible. Finally, we show that an arbitrary action can be reached with positive probability in a finite number of steps.

1. Simulated annealing procedure behaves as a Markov chain

We first establish the preliminaries of the simulated annealing procedure used in DNC, which is necessary to describe the procedure as a Markov chain [cf. Bertsimas and Tsitsiklis, 1993].

1. \mathcal{A} is a finite discrete action set.
2. There exists a real-valued cost function $Q^\pi: \mathcal{S} \times \mathcal{A} \mapsto \mathbb{R}$, with a proper subset of local minima $\mathcal{A}^* \subset \mathcal{A}$. Specifically, we associate each state-action pair with an estimated Q -value $Q_w(\mathbf{s}, \mathbf{a}) \in \mathbb{R}$. Since state \mathbf{s} is fixed while executing the simulated annealing algorithm, we omit its notation moving forward.
3. Every action $\mathbf{a} \in \mathcal{A}$ has a non-empty neighborhood $\mathcal{A}_{\mathbf{a}} \subseteq \mathcal{A}$ that includes itself, such that $|\mathcal{A}_{\mathbf{a}}| > 1$. This can be ensured by setting an appropriate maximum perturbation distance $(d\epsilon) \in \mathbb{R}^+$. As DNC performs perturbations on each individual entry in the action vector, it follows that all feasible entries (and thus all actions) in the finite action space can be constructed through perturbation of neighboring entries. Finally, given that the Euclidean distance is a symmetric metric, it follows that $\mathbf{a}' \in \mathcal{A}_{\mathbf{a}} \iff \mathbf{a} \in \mathcal{A}_{\mathbf{a}'}$.
4. When we find non-improving neighbors k_1 – which happens in finite time given that the action space is finite – there exists a set of positive probabilities $p_{\mathbf{a}, \mathbf{a}'}, \mathbf{a} \neq \mathbf{a}'$ that reflect the probability of evaluating neighbor \mathbf{a}' from \mathbf{a} . The sum of probabilities satisfies $\sum_{\mathbf{a}' \in \mathcal{A} \setminus \{\mathbf{a}\}} p_{\mathbf{a}, \mathbf{a}'} = 1$. Specifically, in (I.14) of Algorithm 1, we associate $\frac{1}{|\mathcal{K}|}$ to each $k_{\text{rand}} \in \mathcal{K}$. As mentioned, we always reach (I.14) in finite time, due to the guarantee of finding non-improving actions in a finite space.
5. There is a temperature scheme $\beta: \mathbb{N} \mapsto (0, \infty)$, with β_t representing temperature at time $t \in \mathbb{N}$ and $\beta_t \geq \beta_{t+1}, \forall t$. Similarly, the scheme $k: \mathbb{N} \mapsto [0, |\mathcal{A}|]$ returns the number of neighbors

k_t generated at time t , with $k_t \geq k_{t+1}, \forall t$. As a preliminary for the remainder of the proof, the temperature must cool sufficiently slow to allow finite-time transitions between any $\mathbf{a}, \mathbf{a}' \in \mathcal{A}$.

6. At $t=0$, an initial action $\bar{\mathbf{a}}$ is given. This action is generated by the continuous-to-discrete mapping function $g: \hat{\mathbf{a}} \mapsto \bar{\mathbf{a}}$, as detailed in the paper.

Given these preliminaries, we define the simulated annealing procedure used in our DNC as a non-homogeneous Markov chain $A = A_0, A_1, A_2, \dots$ that searches over \mathcal{A} . Here, A_t is a random variable that denotes the accepted action after move t , i.e., $A_t = \mathbf{a}_t, \mathbf{a}_t \in \mathcal{A}$. Let us denote $\mathbf{k}_1 = \underset{\mathbf{k} \in \mathcal{K}'}{\operatorname{argmax}} (Q(\mathbf{s}, \mathbf{k}))$ and $\kappa = \max \left(0, \frac{Q(\mathbf{s}, \mathbf{a}) - Q(\mathbf{s}, \mathbf{k}_1)}{\beta} \right)$. Then, from the algorithmic outline, we derive that the probability of $A_{t+1} = \mathbf{a}'$ when $A_t = \mathbf{a}$ is given by

$$\mathbb{P}(A_{t+1} = \mathbf{a}' | A_t = \mathbf{a}) = \begin{cases} \exp(\kappa) + (1 - \exp(\kappa)) \cdot \frac{1}{|\mathcal{K}|}, & \text{if } \mathbf{a}' = \mathbf{k}_1 \\ (1 - \exp(\kappa)) \cdot \frac{1}{|\mathcal{K}|}, & \text{if } \mathbf{a}' \neq \mathbf{k}_1 \end{cases} \quad (2)$$

2. Markov chain is irreducible and aperiodic

We now show that the transition probabilities of the Markov chain imply it is (i) irreducible and (ii) aperiodic, which are necessary and sufficient conditions to prove that $\mathbb{P}(A_{t+\tau} = \mathbf{a}' | A_t = \mathbf{a}) > 0$ for some finite $\tau \in \mathbb{N}$.

- (i) *Irreducibility of A* : To show that the Markov chain is irreducible, suppose we set the maximum perturbation distance to $(d\epsilon) = \max_{\mathbf{a}, \mathbf{a}' \in \mathcal{A}} \|\mathbf{a} - \mathbf{a}'\|_2$, i.e., equaling the finite upper bound on perturbation. Now, suppose we wish to move between arbitrary actions $\mathbf{a} = (a_n)_{\forall n \in \{1, \dots, N\}}$ and $\mathbf{a}' = (a'_n)_{\forall n \in \{1, \dots, N\}}$. The chosen perturbation distance ensures that action entries can be perturbed to any target value $a'_n \in \{a_n - (d\epsilon), \dots, a_n + (d\epsilon)\}$. By perturbing each entry a_n individually, we can reach \mathbf{a}' within N steps, as Equation (2) ensures a positive probability of accepting such perturbations. To generalize the established result, observe that we may relax to $(d\epsilon) \leq \max_{\mathbf{a}, \mathbf{a}' \in \mathcal{A}} \|\mathbf{a} - \mathbf{a}'\|_2$ and can construct a similar rationale for some smaller d that satisfies communication between action pairs as well.
- (ii) *Aperiodicity of A* : As we accept non-improving actions with a probability < 1 and $\exists \mathbf{a}^* \in \mathcal{A}^*$ with no improving neighbors, a one-step transition probability $\mathbb{P}(A_{t+1} = \mathbf{a}^* | A_t = \mathbf{a}^*) > 0$ is implied by Equation (2). By definition of aperiodicity, identifying one aperiodic action suffices to prove that the entire Markov chain is aperiodic.

3. All actions are reachable with positive probability in finite time

We have shown that the Markov chain is irreducible and aperiodic, proving that all actions belong to the same communicating class. By the Perron-Frobenius theorem, $\forall (\mathbf{a}, \mathbf{a}')$, there exists a finite τ such that $\mathbb{P}(A_{t+\tau} = \mathbf{a}' | A_t = \mathbf{a}) = (\mathcal{P}^\tau)_{\mathbf{a}\mathbf{a}'} > 0$, where $(\mathcal{P}^\tau)_{\mathbf{a}\mathbf{a}'}$ is a τ -step transition matrix.

This result shows that there is a positive probability of reaching action \mathbf{a}' from action \mathbf{a} in τ steps. Thus, given sufficiently large perturbation distances and an appropriate cooling scheme, DNC enables to find improving actions outside the initial neighborhood. \square

B Environments

Maze Our implementation follows the implementation as described in Chandak et al. [2019]. We set the episode length to 150 steps and provide a reward of -0.05 for each move and 100 for reaching the target. The target, wall, and initial agent position follow the illustration in Figure 3. Here, the red dot represents the agent with the actuators, the blue areas are walls which the agent cannot move through, and the yellow star is the target area. The agent cannot move outside the boundaries of the maze. Whenever a wall or outside boundary is hit, the agent does not move and remains in the same state. Action noise was added to make the problem more challenging. On average 10% of the agent movements are distorted by a noise signal, making the agents' movements result in slightly displaced locations.

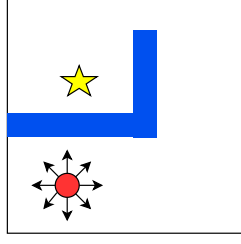


Figure 3: Illustration of the maze environment.

Recommender We base the recommender environment on the data provided in Grouplens [2023]. We use the data file `movies.csv` – which contains 62,424 lines each describing one movie – to construct a feature vector per movie as follows. First, we vectorize the list of movies based on their genre description using a combined *term-frequency* (tf) and *inverse-document-frequency* (idf) vectorizer [cf. Scikit-Learn, 2023]. This results in a $62,424 \times 23$ matrix, denoted by $\mathbf{T}^{\text{tf-idf}} \in \mathbb{R}^{62,424 \times 23}$, where each row is one movie feature vector and contains 23 features. Second, as the resulting matrix contains several duplicates, i.e., movies with the exact same combination of features, we retrieve only unique feature vectors resulting in a reduced $\mathbf{T}^{\text{tf-idf}} \in \mathbb{R}^{1639 \times 23}$ matrix with shape $1,639 \times 23$. Third, we base the conditional probability of a customer picking movie j if the last movie picked was i on the cosine similarity of both movies’ feature vectors. Cosine similarity S_{ij} between two movies i and j is computed as follows

$$S_{ij} = \frac{\mathbf{T}_i^{\text{tf-idf}} \cdot \mathbf{T}_j^{\text{tf-idf}}}{\|\mathbf{T}_i^{\text{tf-idf}}\| \|\mathbf{T}_j^{\text{tf-idf}}\|} . \quad (3)$$

We then obtain a probability \tilde{P}_{ij} of picking recommended movie j – when the last picked movie was i – by applying a sigmoid function to each S_{ij} , yielding

$$\tilde{P}_{ij} = \frac{1}{1 + \exp(-5 \cdot S_{ij})} . \quad (4)$$

We use a multiplier of -5 to ensure that the transition from 0 to 1 is not too steep. Finally we attribute rewards of 1, 10, and 30 to the first 60%, 60%–90%, and last 10% of movies respectively. Here, we note that we do not consider correlations between reward and the associated movie. As reported in the paper, episodes end with probability of 0.1 if the recommended movie gets picked and with 0.2 otherwise. This corresponds to the setting studied in Dulac-Arnold et al. [2015] and simulates user patience.

Inventory Replenishment We mostly follow the implementation as detailed in Vanvuchelen et al. [2022], wherein they consider a retailer managing uncertain demand for different items in its warehouse. Compared to them, we run shorter episodes to decrease the computational burden. The costs per item $i \in \mathcal{I}$ are as follows: holding costs $h_i = 1$, backorder costs $b_i = 19$, ordering costs $o_i = 10$ and the common order costs are $O = 75$. The order-up-to levels are set to the range $[0, 66]$. We sample the demand rate from the Poisson distribution, with half of the items having a demand rate of $\lambda_i = 10$, and the other half of the items $\lambda_i = 20$. We initialize all inventory levels to 25. Every episode comprises 100 timesteps. The reward function can be denoted by:

$$R_t = \sum_{i=1}^N (h_i I_{i,t}^+ + b_i I_{i,t}^- + o_i \mathbb{1}_{\{q_{i,t} > 0\}}) + O \mathbb{1}_{\{\sum_{i=1}^N q_{i,t} > 0\}} , \quad (5)$$

where $I_{i,t}^+$ and $I_{i,t}^-$ indicate all positive and negative stock levels, respectively. $\mathbb{1}_{q_{i,t} > 0}$ is the indicator function for ordering item i , and $\mathbb{1}_{\{\sum_{i=1}^N q_{i,t} > 0\}}$ indicates that at least one product is ordered.

C Implementation Details

Integration of DNC in an actor-critic algorithm Algorithm 2 details the integration of DNC into an actor-critic reinforcement learning (RL) algorithm. Specifically, we initialize the network weights

w and θ of the critic and actor respectively (1.1), and set hyperparameters such as the Gaussian σ and the critic- and actor learning rates α_{cr} and α_{ac} (1.2). After initializing a state s (1.4), we loop through each time step of an episode (1.5). We obtain a continuous action \hat{a} by sampling it from π_θ according to the learned μ_θ and σ of a Gaussian distribution and the hyperparameter θ (1.6). Next, we obtain a discrete action \bar{a}^* by applying DNC (1.7), whose details are provided in Algorithm 1 in the main body of the paper. We then apply \bar{a}^* to the environment, observe reward r and next state s' (1.8). We obtain the next state's continuous action \hat{a}' (1.9) and then its discrete action $\bar{a}^{*'} (1.10)$. Using losses based on the observed TD-error (1.11), we update critic (1.12) and actor (1.13) weights. Note that we use both \hat{a} and a TD-error based on \bar{a}^* and $\bar{a}^{*'}$, hence using slightly off-policy information to compute the actor loss. However, since in practice DNC does not move far away from \hat{a} , using off-policy information in the actor weight update does not heavily impact on learning stability.

Algorithm 2 Actor critic pseudo-code with DNC.

```

1: Initialize network weights  $w, \theta$ 
2: Set hyperparameters:  $\sigma, \alpha_{cr}, \alpha_{ac}$ 
3: for each episode do
4:   Initialize  $s$ 
5:   for each time step  $t$  do
6:      $\hat{a} \leftarrow \pi_\theta(s)$  (based on  $\sigma$ )
7:      $\bar{a}^* = \text{DNC}(\hat{a})$  (see Algorithm 1)
8:     Apply  $\bar{a}^*$  to environment, observe reward  $r$ , and successor state  $s'$ 
9:      $\hat{a}' \leftarrow \pi_\theta(s')$  (based on  $\sigma$ )
10:     $\bar{a}^{*' } = \text{DNC}(\hat{a}')$ 
11:     $\delta = r + \gamma Q(s', \bar{a}^{*' }, w) - Q(s, \bar{a}^*, w)$ 
12:     $w \leftarrow w - \alpha_{cr} \nabla_w \delta$ 
13:     $\theta \leftarrow \theta + \alpha_{ac} \delta \nabla_\theta \log \pi_\theta(s, \hat{a})$ 

```

Details on the Neural Network Architecture When applying a deep network architecture, we use two hidden layers with ReLU activation functions for both actor and critic for DNC and all benchmarks. In Section E we provide further details for the architecture per environment. For all environments, we use a tanh output layer for the actor and do not bound the output of the critic.

We train the actor and critic based on the stochastic gradient descent algorithm implemented in PyTorch and use a Huber loss to train the critic and ensure stable weight updates.

Recommender Specific Implementation Details The movie features, i.e., values of $T^{\text{tf-idf}}$, are between 0 and 1. To obtain discrete values, we round each value to two decimal places and set ϵ to values between 0.01 and 0.1. With this discretization, DNC and MinMax (MinMax) potentially return non-existent actions, i.e., recommend non-existent movies. Hence, the output \bar{a}^* of DNC and MinMax may be infeasible. Therefore, after obtaining \bar{a}^* , a feasibility check is required to find an existent action closest to \bar{a}^* . In our case, we employ FLANN [Muja and Lowe, 2014] to find an existing action in $T^{\text{tf-idf}}$. However, different feasibility checks could be employed as alternative. Note that, opposed to knn which also employs FLANN, the feasible action search complexity only increases linearly in the number of movies. This is because we search for neighbors directly in the $T^{\text{tf-idf}}$ matrix, whereas knn would search for neighbors in the complete action space \mathcal{A} , i.e., a search in a 1639×23 sized matrix versus a search in a matrix with over one million elements.

Other Implementation Details We employ a discretization function $g(\hat{a})$ to obtain a discrete base action \bar{a} from the continuous action \hat{a} . The discretization function has multiple hyperparameters that need to be selected based on (i) the output layer activation function, and (ii) the action dimension. These hyperparameters are $c_{\min}, c_{\max}, a_{\min}$, and a_{\max} , which clip and subsequently normalize the action before rounding to the nearest integer. Since the action is sampled from a distribution, an action might overflow and result in non-existent actions, hence, clipping is required. Each value needs to be set to an appropriate value. We use $c_{\min} = -1, c_{\max} = 1$ for clipping, since we employ a tanh activation function for the output layer. The values for a_{\min} and a_{\max} are set depending on the environment; we use $[0, 1]$ for maze and recommender, and $[0, 66]$ for the inventory environment.

We represent states across all environments by means of a Fourier basis as described in Konidaris et al. [2011] and applied in Chandak et al. [2019]. In the maze environment we use a Fourier basis of order three with coupled terms. For the recommender and inventory environments, we use decoupled terms to maintain a reasonable state vector size.

D Benchmarks

We consider four benchmarks: VAC, MinMax, knn , and LAR. For a full and detailed explanation of the benchmarks, we refer to Sutton and Barto [2018], Vanvuchelen et al. [2022], Dulac-Arnold et al. [2015], and Chandak et al. [2019], respectively. Here, we restrict ourselves to a short description of each benchmark and explain how we embed these benchmarks in an actor-critic algorithm similar to Algorithm 2.

VAC We employ a standard actor-critic method as benchmark. For this method we employ a categorical policy, i.e., π describes the probability of taking action a when being in state s . We denote the policy by $\pi(a|s)$ to emphasize that π is a distribution. VAC’s implementation follows Algorithm 2, as detailed above, with the only difference that we obtain the discrete action directly from the actor, instead of obtaining a continuous action and subsequently using DNC.

MinMax The MinMax benchmark uses an actor-critic framework, in which the actor outputs a continuous action vector and function g is applied in the same way as for DNC. We obtain the algorithm corresponding to MinMax by exchanging DNC in lines 7 and 10 of Algorithm 2 by g .

knn The knn approach uses an approximate nearest neighbor lookup [Muja and Lowe, 2014] to find discrete neighbors in the space \mathcal{A} based on continuous action \hat{a} . The mapping function h finds the k nearest discrete neighbors in terms of Euclidean distance:

$$h_k(\hat{a}) = \arg \min_{a \in \mathcal{A}^k} \|a - \hat{a}\|_2.$$

After finding k neighbors, the neighbor with highest Q -value is chosen and applied to the environment, using a similar approximate on-policy rationale as applied for DNC. Note that the critic is only used to select an action *after* all neighbors have been generated. In Section E we present different values of k , over which we search for the best performing hyperparameter setting for knn . To embed knn in an actor-critic algorithm, we modify Algorithm 2 in lines 7 and 10 as follows: instead of applying DNC, we search for the k -nearest neighbors of \hat{a} and \hat{a}' , and, subsequently, obtain \bar{a}^* and $\bar{a}^{*'} by selecting the neighbor with highest Q -value.$

LAR To setup the LAR benchmark, we use the code that implements the work presented in Chandak et al. [2019] and that was kindly shared with us. In the following we briefly describe the algorithm. Before training the RL agent, we apply an initial supervised learning process to learn unique action embeddings $e' \in \mathbb{R}^l$ for each discrete action a . We use a buffer that stores state, action, and successor state transition data to feed the supervised learning model. We set the maximum buffer size to 6e5 transitions and obtain these transitions from, e.g., a random policy. The supervised loss is determined using the KL-divergence between the true distribution $P(a_t|s_t, s_{t+1})$ and the estimated distribution $\hat{P}(a_t|s_t, s_{t+1})$, which describe probabilities of taking an action a_t at time step t when having a certain state tuple (s_t, s_{t+1}) . Across all environments, we use a maximum of 3000 epochs to minimize the supervised loss. We note here that the training process always converged before reaching the 3000 epochs limit. We detail the different sizes of the two-layer neural network architecture, used in the supervised learning procedure, in Section E. Moreover, note that the size of e may be both larger or smaller than the discrete action’s size. It is up to the user to determine the embedding size, hence, it is a hyperparameter whose values we also report in Section E.

Following the initial supervised learning process, we proceed in a similar manner to Algorithm 2. First, we obtain e from the continuous policy π (cf. line 6 in Algorithm 2). Second, we find the embedding e' closest to e based on an L_2 distance metric and look up the discrete action a corresponding to e' (cf. line 7 in Algorithm 2). At the end of each step of the episode, we update the continuous representations e' of a by performing one supervised learning step.

E Hyperparameters

In this section, we detail the hyperparameter settings used across the different environments. To this end, we provide an overview of hyperparameter settings in Table 2 and discuss specific settings that we use over all environments. N/A indicates that the respective method did not yield a performant policy for any hyperparameter setting.

We applied a search over the reported set of values in Table 2 (column "Set of values") to choose the best hyperparameter setting. Note that a value of zero nodes of the critic and actor layer corresponds to a shallow network. Moreover, we do not report hyperparameter settings for MinMax separately, as its only hyperparameter corresponds to c_{\min} and c_{\max} , which we set to the minimum, resp. maximum value of the actor’s output layer as described in Section C.

For all environments, we chose the actor’s learning rate to be $10\times$ smaller than the critic’s rate to ensure that the values provided by the critic are up-to-date.

We study both (i) learning the second moment of the Gaussian distribution, σ , and (ii) setting σ to a constant value. In Table 2, a \dagger indicates that σ was learned by the actor. We found that a constant σ often led to faster convergence without performance loss.

The DNC-specific parameters are (i) the neighborhood depth d , (ii) the k -best neighbors to consider, (iii) the acceptance probability parameter β , and (iv) the cooling parameter c . We do not tune β , and set it to an initial value of 0.99. The cooling parameter expresses by how much the parameter k and β are decreased every iteration of the search, in terms of percentage of the initial values of both parameters. We set k respective to the size of neighborhood $|\mathcal{A}'|$.

Table 2: Hyperparameters, set of values, and chosen values.

Hyperparameters		Set of values	Chosen values		
			Maze	Recommender	Inventory
Overall	α_{cr} (critic learning rate)	$\{10^{-2}, 10^{-3}, 10^{-4}\}$	10^{-2}	10^{-3}	10^{-2}
	α_{ac} (actor learning rate)	$\{10^{-3}, 10^{-4}, 10^{-5}\}$	10^{-2}	10^{-4}	10^{-3}
	σ	$\{\dagger, 0.25, 0.5, 1\}$	1	0.25	0.5
	# actor NN nodes/layer	$\{0, 32, 64, 128\}$	0	0	32
	# critic NN nodes/layer	$\{0, 32, 64, 128\}$	32	64	64
LAR	$ e $	$\{0.5 s , s , 2 s \}$	$ s $	$ s $	N/A
	# supervised NN nodes	$\{0, 64\}$	0	0/64	N/A
knn	k	$\{1, 2, 20, 100\}$	2	20	N/A
DNC	d	$\{1, 2, 5, 10\}$	1	5	1
	k	$\{10\%, 50\%\}$	10%	10%	10%
	c	$\{10\%, 25\%, 50\%, 75\%\}$	25%	25%	25%

F Complementary Results

In this section, we provide additional result plots and interpretation. Figure 4 depicts the performance of the converged policies over the 10 training seeds. The left column depicts results for the maze environment. For the 12 actuator variant, all policies except VAC converge to the target without too much variance between seeds. For the larger 28 actuator variant, we observe that both policies have a large variance, i.e., not all training runs converge to a performant policy, taking a short path to the goal. As discussed in the main text, the benefit of considering neighbors is limited for the maze environment. The variance of DNC over training seeds is larger due to the neighborhood search.

The middle column shows results for the recommender environment. Here, we see for the case with one recommended item that LAR finds the best policy with smallest variance, closely followed by DNC, which has more variance. knn and VAC find similar performing policies, although knn shows less variance among training seeds. MinMax does not find a performant policy. For the larger case with two recommended items, VAC, LAR, and MinMax fail to find a performant policy, whereas

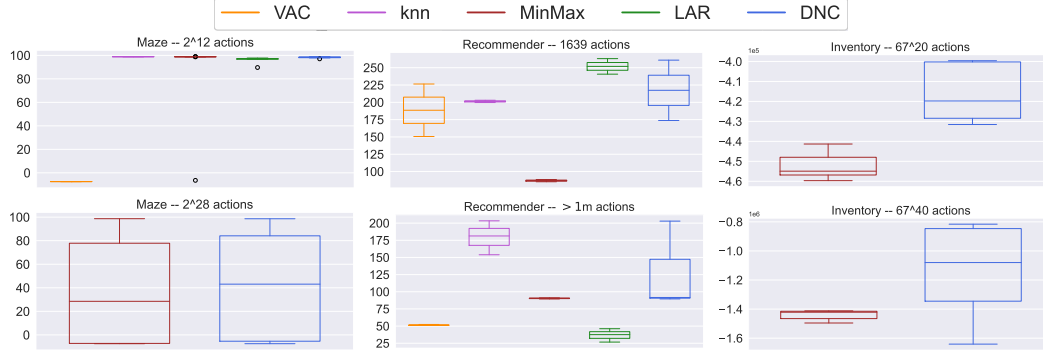


Figure 4: Average total expected returns of the converged policies over 10 random seeds. The boxplots show the median, interquartile range, and outliers. (Top) smaller action space variants of the three studied environments. (Bottom) larger action space variants for the three studied environments.

knn and DNC do find performant policies. The benefit of searching for neighbors is apparent by the difference in performance of DNC and MinMax.

The right column shows results for the inventory environment. Here, we observe for both settings that DNC outperforms MinMax. The larger variance of DNC compared to MinMax is explained by the neighborhood search.

We visually compare policies for the maze environment. Figure 5 shows exploration heatmaps for all methods for the 12 actuator setting of the maze environment. Here, the more frequently a location is visited, the brighter the color, i.e., from least visits to most visits: black-red-orange-yellow. We note that at the start of training, the movement of the agent is still random. However, as the policies

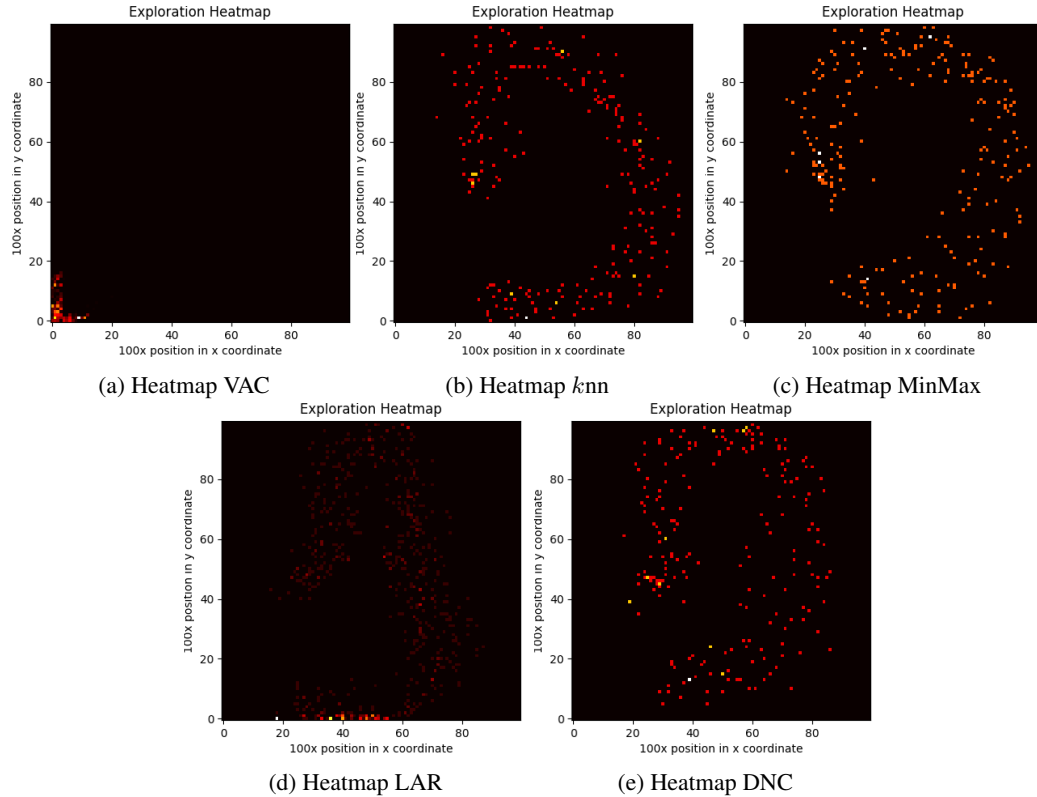


Figure 5: Exploration heatmap over all training episodes of each method for the 12 actuator case.

converge, a clearer path becomes visible, given the 10% action noise. VAC is unable to handle the large action space and gets stuck in the lower left corner. *knn* and MinMax eventually find a comparable policy that reaches the goal state, albeit the shortest path is not found. It seems that both policies learned to stay far away from the wall, as hitting the wall often results in getting stuck. Both LAR and DNC found a policy that tracks more closely around the wall, hence taking a shorter path to the goal state. However, LAR remained at the lower boundary of the grid for some episodes.

G Computational Resources

Our experiments are conducted on a high-performance cluster with 2.6Ghz CPUs with 56 threads and 64gb RAM per node. The algorithms are coded in Python 3 and we use PyTorch to construct neural network architectures [Paszke et al., 2019]. For the maze environment, having relatively long episodes, the average training time was 21 CPU hours. For the recommender environment, training times were approximately 7 CPU hours, and the inventory environment took on average 12 CPU hours to train.

References

- M. Mehdi Afsar, Trafford Crump, and Behrouz Far. Reinforcement learning based recommender systems: A survey. *ACM Comput. Surv.*, 55(7), 2022.
- Dimitris Bertsimas and John Tsitsiklis. Simulated annealing. *Statistical Science*, 8(1):10–15, 1993. ISSN 08834237.
- Robert N. Boute, Joren Gijsbrechts, Willem van Jaarsveld, and Nathalie Vanvuchelen. Deep reinforcement learning for inventory control: A roadmap. *European Journal of Operational Research*, 298(2):401–412, 2022.
- Yash Chandak, Georgios Theodorou, James Kostas, Scott Jordan, and Philip Thomas. Learning action representations for reinforcement learning. In *International conference on machine learning*, pages 941–950. PMLR, 2019.
- Hao Cui and Roni Khordon. Online symbolic gradient-based optimization for factored action mdps. In *International Joint Conference on Artificial Intelligence*, pages 3075–3081. IJCAI/AAAI Press, 2016.
- Hao Cui and Roni Khordon. Lifted stochastic planning, belief propagation and marginal map. In *AAAI Workshops*, volume WS-18 of *AAAI Technical Report*, pages 658–664. AAAI Press, 2018.
- Gabriel Dulac-Arnold, Ludovic Denoyer, Philippe Preux, and Patrick Gallinari. Fast reinforcement learning with large action sets using error-correcting output codes for MDP factorization. In *Joint European Conference on Machine Learning and Knowledge Discovery in Databases*, pages 180–194. Springer, 2012.
- Gabriel Dulac-Arnold, Richard Evans, Hado van Hasselt, Peter Sunehag, Timothy Lillicrap, Jonathan Hunt, Timothy Mann, Theophane Weber, Thomas Degris, and Ben Coppin. Deep reinforcement learning in large discrete action spaces. *arXiv preprint arXiv:1512.07679*, 2015.
- Gabriel Dulac-Arnold, Nir Levine, Daniel J. Mankowitz, Jerry Li, Cosmin Paduraru, Sven Gowal, and Todd Hester. Challenges of real-world reinforcement learning: definitions, benchmarks and analysis. *Machine Learning*, 110(9):2419–2468, Sep 2021.
- Tobias Enders, James Harrison, Marco Pavone, and Maximilian Schiffer. Hybrid multi-agent deep reinforcement learning for autonomous mobility on demand systems. *arXiv preprint arXiv:2212.07313*, 2022.
- Grouplens. Movielens 25m dataset. <https://grouplens.org/datasets/movielens/25m/>, 2023. Accessed: 2023-05-05.
- Pengjie Gu, Mengchen Zhao, Chen Chen, Dong Li, Jianye Hao, and Bo An. Learning pseudometric-based action representations for offline reinforcement learning. In Kamalika Chaudhuri, Stefanie Jegelka, Le Song, Csaba Szepesvari, Gang Niu, and Sivan Sabato, editors, *Proceedings of the 39th International Conference on Machine Learning*, volume 162 of *Proceedings of Machine Learning Research*, pages 7902–7918. PMLR, 17–23 Jul 2022.
- Ji He, Jianshu Chen, Xiaodong He, Jianfeng Gao, Lihong Li, Li Deng, and Mari Ostendorf. Deep reinforcement learning with a natural language action space. In *Proceedings of the 54th Annual Meeting of the Association for Computational Linguistics (Volume 1: Long Papers)*, pages 1621–1630, Berlin, Germany, August 2016. Association for Computational Linguistics.

- Junsu Kim, Younggyo Seo, and Jinwoo Shin. Landmark-guided subgoal generation in hierarchical reinforcement learning. In A. Beygelzimer, Y. Dauphin, P. Liang, and J. Wortman Vaughan, editors, *Advances in Neural Information Processing Systems*, NIPS’21, 2021a.
- Minsu Kim, Jinkyoo Park, and joungho kim. Learning collaborative policies to solve np-hard routing problems. In M. Ranzato, A. Beygelzimer, Y. Dauphin, P.S. Liang, and J. Wortman Vaughan, editors, *Advances in Neural Information Processing Systems*, volume 34, pages 10418–10430. Curran Associates, Inc., 2021b.
- Mykel J. Kochenderfer and Tim A. Wheeler. *Algorithms for Optimization*. The MIT Press, 2019. ISBN 0262039427.
- George Konidaris, Sarah Osentoski, and Philip Thomas. Value function approximation in reinforcement learning using the fourier basis. *Proceedings of the AAAI Conference on Artificial Intelligence*, 25(1):380–385, Aug. 2011.
- Michail Lagoudakis and Ronald Parr. Reinforcement learning as classification: Leveraging modern classifiers. In *Proceedings of the Twentieth International Conference (ICML 2003)*, pages 424–431, 01 2003.
- Anuj Mahajan, Mikayel Samvelyan, Lei Mao, Viktor Makoviyuchuk, Animesh Garg, Jean Kossaifi, Shimon Whiteson, Yuke Zhu, and Animashree Anandkumar. Reinforcement learning in factored action spaces using tensor decompositions, 2021.
- Volodymyr Mnih, Koray Kavukcuoglu, David Silver, Alex Graves, Ioannis Antonoglou, Daan Wierstra, and Martin Riedmiller. Playing atari with deep reinforcement learning, 2013.
- Marius Muja and David G. Lowe. Scalable nearest neighbor algorithms for high dimensional data. *IEEE Transactions on Pattern Analysis and Machine Intelligence*, 36(11):2227–2240, 2014. doi: 10.1109/TPAMI.2014.2321376.
- Adam Paszke, Sam Gross, Francisco Massa, Adam Lerer, James Bradbury, Gregory Chanan, Trevor Killeen, Zeming Lin, Natalia Gimelshein, Luca Antiga, Alban Desmaison, Andreas Köpf, Edward Yang, Zach DeVito, Martin Raison, Alykhan Tejani, Sasank Chilamkurthy, Benoit Steiner, Lu Fang, Junjie Bai, and Soumith Chintala. Pytorch: An imperative style, high-performance deep learning library. In H. Wallach, H. Larochelle, A. Beygelzimer, F. d’Alché-Buc, E. Fox, and R. Garnett, editors, *Proceedings of the 33rd International Conference on Neural Information Processing Systems*, volume 32. Curran Associates, Inc., 8–14 Dec 2019.
- Jason Pavis and Ron Parr. Generalized value functions for large action sets. In *Proceedings of the 28th International Conference on Machine Learning (ICML-11)*, pages 1185–1192, 2011.
- Bei Peng, Tabish Rashid, Christian Schroeder de Witt, Pierre-Alexandre Kamienny, Philip Torr, Wendelin Boehmer, and Shimon Whiteson. Facmac: Factored multi-agent centralised policy gradients. In M. Ranzato, A. Beygelzimer, Y. Dauphin, P.S. Liang, and J. Wortman Vaughan, editors, *Advances in Neural Information Processing Systems*, volume 34, pages 12208–12221. Curran Associates, Inc., 2021.
- Uta Pigorsch and Sebastian Schäfer. High-dimensional stock portfolio trading with deep reinforcement learning, 2021.
- Paul J. Pritz, Liang Ma, and Kin K. Leung. Jointly-learned state-action embedding for efficient reinforcement learning. In *Proceedings of the 30th ACM International Conference on Information & Knowledge Management*, CIKM ’21, page 1447–1456, New York, NY, USA, 2021. Association for Computing Machinery. ISBN 9781450384469. doi: 10.1145/3459637.3482357.
- Brian Sallans and Geoffrey E. Hinton. Reinforcement learning with factored states and actions. *J. Mach. Learn. Res.*, 5:1063–1088, dec 2004. ISSN 1532-4435.
- John Schulman, Filip Wolski, Prafulla Dhariwal, Alec Radford, and Oleg Klimov. Proximal policy optimization algorithms, 2017.
- Scikit-Learn. Scikit-learn tf-idf vectorizer. https://scikit-learn.org/stable/modules/generated/sklearn.feature_extraction.text.TfidfVectorizer.html, 2023. Accessed: 2023-05-05.
- Sahil Sharma, Aravind Suresh, Rahul Ramesh, and Balaraman Ravindran. Learning to factor policies and action-value functions: Factored action space representations for deep reinforcement learning. *CoRR*, abs/1705.07269, 2017. URL <http://arxiv.org/abs/1705.07269>.
- David Silver, Guy Lever, Nicolas Heess, Thomas Degris, Daan Wierstra, and Martin Riedmiller. Deterministic policy gradient algorithms. In Eric P. Xing and Tony Jebara, editors, *Proceedings of the 31st International Conference on Machine Learning*, volume 32 of *Proceedings of Machine Learning Research*, pages 387–395, Beijing, China, 22–24 Jun 2014. PMLR.

- Richard S. Sutton and Andrew G. Barto. *Reinforcement Learning: An Introduction*. The MIT Press, Cambridge, MA, USA, second edition, 2018.
- Shengpu Tang, Maggie Makar, Michael Sjoding, Finale Doshi-Velez, and Jenna Wiens. Leveraging factored action spaces for efficient offline reinforcement learning in healthcare. In Alice H. Oh, Alekh Agarwal, Danielle Belgrave, and Kyunghyun Cho, editors, *Advances in Neural Information Processing Systems*, 2022. URL <https://openreview.net/forum?id=Jd70afzIvJ4>.
- Arash Tavakoli, Fabio Pardo, and Petar Kormushev. Action branching architectures for deep reinforcement learning. In *Proceedings of the Thirty-Second AAAI Conference on Artificial Intelligence and Thirtieth Innovative Applications of Artificial Intelligence Conference and Eighth AAAI Symposium on Educational Advances in Artificial Intelligence*, AAAI’18/IAAI’18/EAAI’18. AAAI Press, 2018. ISBN 978-1-57735-800-8.
- Guy Tennenholtz and Shie Mannor. The natural language of actions. In Kamalika Chaudhuri and Ruslan Salakhutdinov, editors, *Proceedings of the 36th International Conference on Machine Learning*, volume 97 of *Proceedings of Machine Learning Research*, pages 6196–6205. PMLR, 09–15 Jun 2019. URL <https://proceedings.mlr.press/v97/tennenholtz19a.html>.
- Philip S. Thomas and Andrew G. Barto. Motor primitive discovery. In *2012 IEEE International Conference on Development and Learning and Epigenetic Robotics (ICDL)*, pages 1–8, 2012. doi: 10.1109/DevLrn.2012.6400845.
- Hado Van Hasselt and Marco A Wiering. Reinforcement learning in continuous action spaces. In *2007 IEEE International Symposium on Approximate Dynamic Programming and Reinforcement Learning*, pages 272–279. IEEE, 2007.
- Nathalie Vanvuchelen, Bram de Moor, and Robert N. Boute. The use of continuous action representations to scale deep reinforcement learning for inventory control. *SSRN*, 10 2022. <https://dx.doi.org/10.2139/ssrn.4253600>.
- Gongju Wang, Dianxi Shi, Chao Xue, Hao Jiang, and Yajie Wang. Bic-ddpg: Bidirectionally-coordinated nets for deep multi-agent reinforcement learning. In Honghao Gao, Xinheng Wang, Muddesar Iqbal, Yuyu Yin, Jianwei Yin, and Ning Gu, editors, *Collaborative Computing: Networking, Applications and Worksharing*, pages 337–354, Cham, 2021. Springer International Publishing.
- Fengsheng Wei, Gang Feng, Yao Sun, Yatong Wang, Shuang Qin, and Ying-Chang Liang. Network slice reconfiguration by exploiting deep reinforcement learning with large action space. *IEEE Transactions on Network and Service Management*, 17(4):2197–2211, 2020.
- William Whitney, Rajat Agarwal, Kyunghyun Cho, and Abhinav Gupta. Dynamics-aware embeddings. In *International Conference on Learning Representations*, 2020. URL <https://openreview.net/forum?id=BJgZGeHFFH>.
- Tom Zahavy, Matan Haroush, Nadav Merlis, Daniel J Mankowitz, and Shie Mannor. Learn what not to learn: Action elimination with deep reinforcement learning. In S. Bengio, H. Wallach, H. Larochelle, K. Grauman, N. Cesa-Bianchi, and R. Garnett, editors, *Advances in Neural Information Processing Systems*, volume 31. Curran Associates, Inc., 2018. URL https://proceedings.neurips.cc/paper_files/paper/2018/file/645098b086d2f9e1e0e939c27f9f2d6f-Paper.pdf.
- Tianren Zhang, Shangqi Guo, Tian Tan, Xiaolin Hu, and Feng Chen. Generating adjacency-constrained subgoals in hierarchical reinforcement learning. In *Proceedings of the 34th International Conference on Neural Information Processing Systems*, NIPS’20, Red Hook, NY, USA, 2020. Curran Associates Inc. ISBN 9781713829546.